

SUPPLEMENTARY INFORMATION

1. Numerical model

1.1. *Supplementary methods*

We solved Equation (1) forward in time on a regular grid with periodic x boundaries and $\nabla^2 z$, ∇z , $U = 0$ at the y boundaries, equivalent to a ridgeline bounded by two streams with constant elevation. The initial condition was a randomly rough surface with relief approximately 100 times lower than the final surface, and iteration proceeded until $\partial z/\partial t = 0$ for all (x,y) . Grids ranged from 300×80 to 300×250 points ($x \times y$) with a point spacing of 0.2 to 20 m. Model solutions with the range of L_c shown in Fig. 2 were obtained by varying D and K .

1.2. *Avoiding resolution effects*

Drainage area in landscape evolution models tends to become concentrated in valleys along paths one grid cell wide. If no steps are taken to compensate for this effect, the steady-state topography for a given set of rate parameters can depend on the spatial resolution of the finite difference grid. To prevent the modelled valley spacing from being resolution-dependent, we smoothed the drainage area field with a square moving average kernel at each time step. For filters wider than a few grid points but narrower than the valleys, valley spacing is only weakly dependent on grid resolution and filter size (Fig. S1). The magnitude of this dependence is comparable to the variability among runs resulting from different initial surfaces. We performed numerical experiments, like that summarized in Fig. S1, to identify the range of acceptable filter sizes for each parameter combination used to construct the blue trend in Fig. 2, and to confirm that the trend is insensitive to spatial resolution. This method for avoiding resolution effects differs from that used in some previous studies of landscape evolution^{8,23}, but is more broadly applicable.

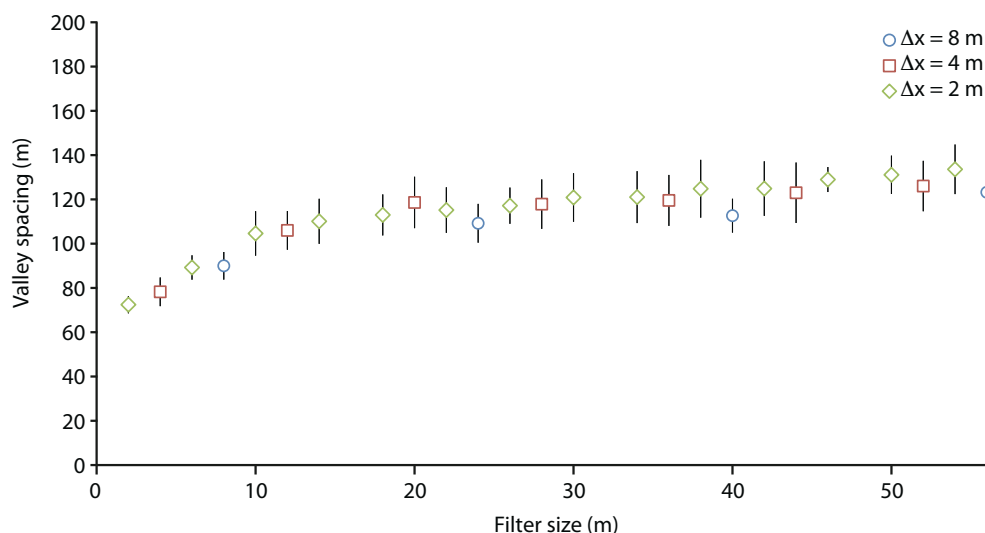


Figure S1. Effects of grid resolution on valley spacing. Plot of modelled valley spacing as a function of drainage area filter size for a range of grid resolutions. Filter sizes correspond to odd numbers of grid points (Δx , $3\Delta x$, $5\Delta x$...). Each point is the mean valley spacing for a set of model runs with $L_c = 10.7$ m. Error bars are 2σ .

2. Topographic measurements

2.1. Supplementary methods

Figure S2 shows the topographic measurements used to calculate L_c for the field sites discussed in the main text. We performed topographic analyses on gridded elevations with a horizontal point spacing of 1 m. We calculated the gradient and Laplacian of elevation from the coefficients of a least-squares quadratic fit to the points within a 7 m radius. The hilltop Laplacian, $\nabla^2 z_h$, was calculated from the mean values within logarithmically spaced bins over the range of $A|\nabla z|$ for which the binned Laplacian was roughly constant (Fig. 3a).

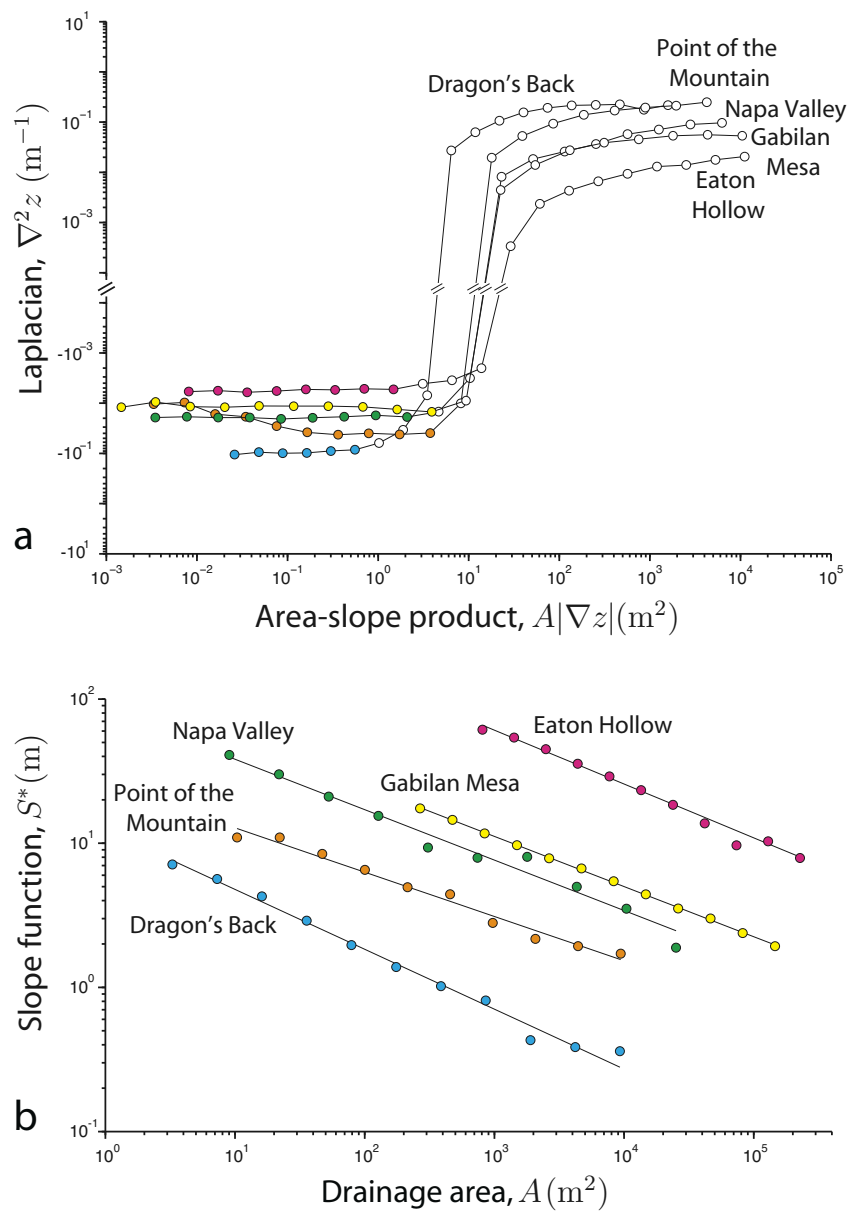


Figure S2. Measurement of model parameters from topography. **a**, Plot of the Laplacian of elevation against the product of drainage area and slope. Circles are means of log-transformed data within logarithmically spaced bins. Coloured circles are the points used to measure $\nabla^2 z_h$. **b**, Plot of slope function (Equation 5, Methods) against drainage area. Circles are means of log-transformed data within logarithmically spaced bins, and lines are least-squares fits to the binned data.

We mapped the drainage network by starting at a threshold drainage area, which was determined by the square of the wavelength at which a kink in the power spectrum indicated a rapid decline in topographic roughness⁶, and then routing flow downslope with a steepest-descent algorithm. Network links with no tributaries were identified as first-order streams. Drainage basins were delineated by starting at the basin outlet, defined as the point just upslope of the junction with a second-order stream, and identifying all upslope points that drain to the outlet. Points showing power-law relationships between S^* and A within individual basins were pooled, and D/K and m were calculated from an iteratively reweighted least-squares fit to the mean values of $\log_{10}(S^*)$ within bins spaced logarithmically in A (Fig. 3b). Uncertainties in L_c were calculated from the uncertainties in D/K , m , and $\nabla^2 z_h$.

2.2. Test of topographic measurement procedure

To verify that our method for inferring L_c from high-resolution topographic data can yield a negative result—i.e., a value of L_c that is inconsistent with the relationship between valley spacing and L_c predicted by the numerical model—we applied the measurement procedure to three landscapes shaped by erosional processes that are not well described by the model (Fig. S3). The Zabriskie Point badlands in Death Valley, California, consist of eroded mudstone with a mean valley spacing of 12 ± 3 m, and are completely unvegetated due to highly arid conditions. The steep, nearly planar slopes and sharp drainage divides indicate that hillslope soil transport at Zabriskie Point is dominated by nonlinear creep^{31,32}, which is not well described by the linear diffusive term in Equation (1). Mettman Ridge in the Oregon Coast Range is a mountainous landscape underlain by sandstone, formerly forested but recently clear-cut, with a valley spacing of 42 ± 12 m. It is a well-documented example of a landscape influenced by nonlinear soil creep³¹, with straight slopes and sharp divides similar to those at Zabriskie point. In addition, valley incision in the Oregon Coast Range is known to be strongly influenced by shallow landslides, debris flows³³⁻³⁷ and, in some locations, deep-seated landslides³⁸, processes for which no well-documented laws for long-term sediment flux exist, and which therefore are not included in our numerical model. Dark Canyon, which lies within the drainage basin of the south fork of the Eel River in California, is a forested landscape underlain by sandstone and mudstone, and has a

valley spacing of 176 ± 9 m (ref. 6). Like Mettman Ridge, Dark Canyon is steep and experiences both nonlinear soil creep and valley incision by debris flows. Parts of the Eel River basin are strongly affected by deep-seated landslides³⁹ and earthflows⁴⁰. We therefore do not expect the valley spacing at these three sites to be consistent with the scaling relationship in Fig. 2.

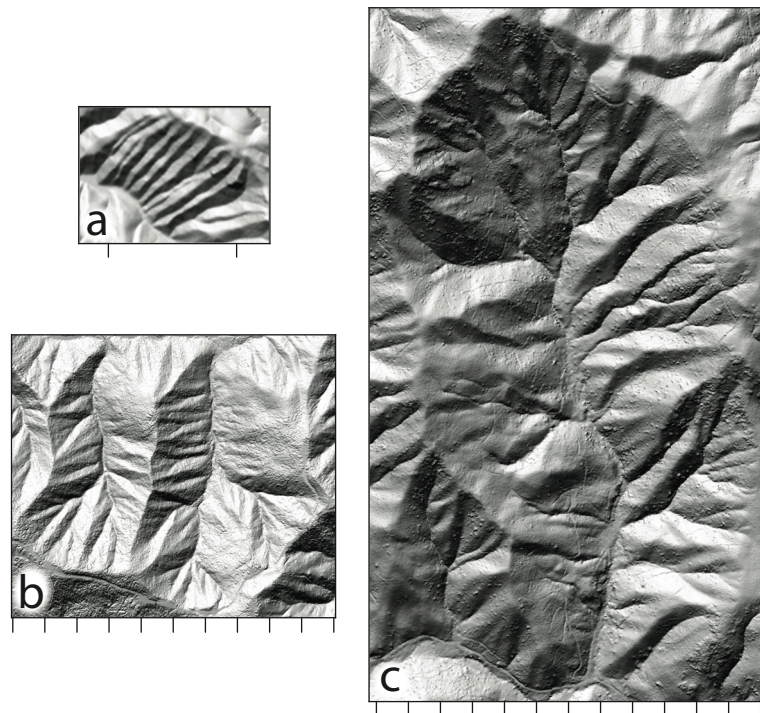


Figure S3. Shaded relief maps of sites with nonlinear soil creep. **a**, Zabriskie Point, California, **b**, Mettman Ridge, Oregon, **c**, Dark Canyon, California. Tick spacing is 100 m. For clarity, **a** has been enlarged by a factor of 4 relative to **b** and **c**. Laser altimetry data for Zabriskie Point and Dark Canyon are from the National Center for Airborne Laser Mapping (NCALM).

Analysing the topography at Zabriskie Point, Mettman Ridge, and Dark Canyon with the same procedure used for the other study sites, we obtain the values in Table S1. For Zabriskie Point, with $L_c = 2.9$ m, the relationship in Fig. 2 predicts a valley spacing between 19 and 37 m, wider than the observed spacing of 12 ± 3 m. The result for Mettman Ridge is similar: for $L_c = 9.1$ m, the relationship in Fig. 2 predicts a valley spacing between 59 and 116 m, wider than the observed spacing of 42 ± 12 m. For Dark Canyon, in contrast, the predicted valley spacing of 84 to 166 m for $L_c = 13.0$ m is narrower than the observed spacing of 176 ± 9 . The overprediction of valley spacing at

Table S1. Topographic measurements for sites with nonlinear creep

	$\nabla^2 z_h$ ($m^{-1} \times 10^{-3}$)	D/K (m^{2m+1})	m	L_c (m)	Observed λ (m)	Predicted λ (m)
Zabriskie Point	-218 ± 19	7 ± 0.4	0.41 ± 0.01	2.9 ± 0.1	12 ± 3	19 – 37
Mettman Ridge	-71 ± 4	26 ± 2	0.24 ± 0.01	9.1 ± 0.7	42 ± 12	59 – 116
Dark Canyon	-30 ± 2	50 ± 3	0.26 ± 0.01	13.0 ± 0.8	176 ± 9	84 – 166

Zabriskie point and Mettman Ridge suggests that valley spacing in landscapes shaped by nonlinear soil creep may be narrower than in landscapes shaped by linear creep. The underprediction at Dark Canyon may be due to the influence of mass wasting processes such as earthflows or deep-seated landslides, which have the demonstrated effect of altering the distribution of topographic variance with respect to wavelength⁴¹. We conclude from our analysis of these three sites that our method for inferring L_c from topographic data is capable of identifying landscapes that have uniform valley spacing but are inconsistent with the model prediction.

Additional References

31. Roering, J. J., Kirchner, J. W. & Dietrich, W. E., Evidence for nonlinear, diffusive sediment transport on hillslopes and implications for landscape morphology. *Water Res. Res.* **35**, 853-870 (1999).
32. Dietrich, W. E. & Perron, J. T., The search for a topographic signature of life. *Nature* **439**, 411-418 (2006).
33. Dietrich, W. E., Wilson, C. J. & Reneau, S. L., Hollows, colluvium, and landslides in soil-mantled landscapes. In *Hillslope Processes* (ed. A. D. Abrahams) 361-388 (Allen & Unwin, London, 1986).
34. Benda, L., Influence of Debris Flows on Channels and Valley Floors in the Oregon Coast Range, U. S. A. *Earth Surf. Process. Landf.* **15**, 457-466 (1990).
35. Stock, J. & Dietrich, W. E., Valley incision by debris flows: Evidence of a topographic signature. *Water Res. Res.* **39**, 1089, doi:10.1029/2001WR001057 (2003).
36. Stock, J. D., Montgomery, D. R., Collins, B. D., Dietrich, W. E. & Sklar, L., Field measurements of incision rates following bedrock exposure: Implications for process controls on the long profiles of valleys cut by rivers and debris flows. *Geol. Soc. Am. Bull.* **117**, 174-194 (2005).

37. Stock, J. & Dietrich, W., Erosion of steepland valleys by debris flows. *Geol. Soc. Am. Bull.* **118**, 1125-1148 (2006).
38. Roering, J. J., Kirchner, J. W. & Dietrich, W. E., Characterizing structural and lithologic controls on deep-seated landsliding: Implications for topographic relief and landscape evolution in the Oregon Coast Range, USA. *Geol. Soc. Am. Bull.* **117**, 654-668 (2005).
39. Mackey, B. H., Roering, J. J., McKean, J. & Dietrich, W. E., Analyzing the Spatial Pattern of Deep-Seated Landsliding—Evidence for Base Level Control, South Fork Eel River, California. *EOS Trans. AGU* **87**, H53B0619 (2006).
40. Mackey, B. H., Roering, J. J. & McKean, J. A., A Hot Knife Through Ice-Cream: Earthflow Response to Channel Incision (Or Channel Response to Earthflows?), Eel River Canyon, California. *Eos, Trans. AGU* **88**, H43H05 (2007).
41. Booth, A. M., Roering, J. J. & Perron, J. T., Automated landslide mapping using spectral analysis and high-resolution topographic data: Puget Sound lowlands, Washington, and Portland Hills, Oregon. *Geomorphology*, in press (2009).